Agromet 38 (2): 78-87, 2024

Agromet
journal.ipb.ac.id/index.php/agromet
ISSN : 0126 - 3633

ENSO and IOD Influence on Extreme Rainfall in Indonesia: Historical and Future Analysis

Risyda Hanifa and Joko Wiratmo
Department of Meteorology, Bandung Institute of Technology, Bandung, 40132

ARTICLE INFO

Received
24 July 2024

Revised
30 September 2024

Accepted for Publication
06 December 2024

Published
16 December 2024

doi: 10.29244/j.agromet.38.2.78-87

Correspondence:
Joko Wiratmo
Department of Meteorology, Bandung Institute of Technology, Bandung, 40132
Email: joko.wiratmo@meteo.itb.ac.id

ABSTRACT

Indonesia, as a maritime continent, is vulnerable to environmental disasters such as floods and landslides due to extreme rainfall. This study aims to identify changes in the influence of ENSO and IOD on extreme rainfall across Indonesia, specifically during the September-October-November period. We used rainfall and sea surface temperature data from the CMIP6 climate model for the historical period (1985-2014), near-future (2031-2060), and far-future (2061-2090) projections under SSP2-4.5 and SSP 5-8.5 climate scenarios. The relation between rainfall dan ENSO/IOD was simply defined by linear regression approach. We analyzed the change of influence by comparing the historical and the future condition. The results indicated that the changes in the teleconnection of ENSO and IOD to extreme rainfall in future is consistently negative, except for Java (near-future) and Kalimantan and southern Sumatra (far-future). Our finding revealed that significant changes in the teleconnection varied throughout maritime continent. The maximum change was found in Northern Kalimantan, which reached values of -80 mm/°C due to ENSO and -180 mm/°C due to IOD for near future. These findings highlight the spatial variability in teleconnection changes across Indonesia, underscoring the need for region-specific climate adaptation measures in response to evolving extreme rainfall patterns.

KEYWORDS
climate projection, linear regression, maritime continent, teleconnection, variability

1. INTRODUCTION

Indonesian maritime continent (IMC) is vulnerable to environmental disaster caused by extreme rainfall, such as floods and landslides, which has significant impact on society (Lestari et al., 2019). As part of the Maritime Continent, crossed by the equator and situated between the Indian and Pacific Oceans, Indonesia is highly susceptible to climate change. Variability in sea surface temperature (SST) influences rainfall characteristics, which can be classified into three distinct regions (Susanto and Aldrian, 2003). Research shows extreme rainfall is projected to increase (Kurniadi et al., 2024) with variation between hemisphere and seasons. Understanding the variability of extreme rainfall is essential for addressing the impacts of floods, droughts, and other hydro-meteorological disasters, which are expected to intensify due to ongoing global warming (Kurniadi et al., 2021).

Over the past two decades, the IMC region has experienced extreme weather and climate events in response to variations in El Niño-Southern Oscillation (ENSO) and Indian Ocean Dipole (IOD). For example, studies on the north coast of Java (Hermawan et al., 2022; Lubis et al., 2022), Nusa Tenggara (Saidah et al., 2023) and eastern Indonesia (Yulihastin et al., 2023), have demonstrated the susceptibility of coastal regions to flooding and drought. Other extreme events affecting the IMC include tropical cyclones (e.g., Cyclone Seroja) (Setiawan et al., 2024), the Borneo vortex (Liang et al., 2023; Trismidianto et al., 2023), and peatland fires (Hamdi et al., 2024). The findings of the

studies indicate a correlation between extreme events and global circulation dynamics, such El Niño.

El Niño event has been linked to prolonged drought conditions in tropical peatlands in Indonesia, which causes a reduction in groundwater levels (GWL) and an increase in the frequency of peatland fires (Lisnawati et al., 2022). However, analysis of GWL measurements over a 27-year period in Central Kalimantan peat forests showed the lowest GWL occurring a few weeks before the onset of El Niño and after the peak of the positive IOD (Sulaiman et al., 2023). The findings highlight a complex interaction between the large-scale climate phenomena and local hydrological responses. As a major source of water vapor at the equator, the IMC plays a critical role in shaping global atmospheric circulation. Understanding the IMC's climate dynamics is crucial, as lack of knowledge may lead to biases and systematic errors in regional and global climate models.

Climate variability in the IMC is strongly modulated by interannual phenomena such as the ENSO and IOD (Amirudin et al., 2020; Hidayat and Ando, 2014). The events are driven by anomalies in sea surface temperatures (SST) and associated wind patterns. Future projections indicate that global warming may alter Pacific Ocean SST, leading to a weakened Walker Circulation, a reduced west-east SST gradient, and an increased frequency of extreme El Niño and La Niña events (Cai et al., 2021). Similarly, changes in the Indian Ocean SST may alter easterly winds and accelerate warming in the western basin, although the frequency and amplitude of the IOD may remain unchanged (Cai et al., 2013). The SST changes are expected to significantly influence weather patterns in Indonesia (Cai et al., 2015).

ENSO and IOD events independently affect extreme rainfall in Indonesia. La Niña and negative IOD caused wetter conditions, while El Niño and positive IOD prolonged drier conditions, with the strongest effects observed during the September-October-November (SON) season (Kurniadi et al., 2021). This season marks the beginning of the rainy season in most Indonesia and is critical for disaster preparedness and agricultural activities, such as the planting of rice in major growing regions (Sutardi et al., 2023). Despite extensive research on historical ENSO and IOD impacts, there is limited understanding of how future SST variability will shape extreme rainfall patterns in Indonesia. This paper investigates the teleconnection between climate in the IMC and global circulation, specifically ENSO and IOD, under future climate scenarios. By improving our understanding of the relationships, we can enhance adaptive strategies and mitigation efforts to address the unpredictable hazards and risks posed by climate variability in the region.

2. RESEARCH METHODS

2.1 Data

The data used in this study consists observational data and climate model output. The observational rainfall data was from the Global Precipitation Measurement (GPM) (https://gpm.nasa.gov/data/). The climate model data was derived from the Coupled Model Intercomparison Project 6 (CMIP6), specifically from the models EC-Earth3, TaiESM1, Community Earth System Model version 2 Whole Atmosphere Community Climate Model (CESM2-WACCM), MIROC6 and NorESM2-LM, including parameters for rainfall and sea surface temperature. The climate model's data have spatial resolutions of 100 km × 100 km and 250 km × 250 km, for the prediction.

The study covers three time periods: the historical period (1985–2014), near-future (2031–2060), and far-future (2061–2090). The Earth system processes, including the atmosphere, ocean, sea ice, and land surface, were simulated by EC-Earth3. TaiESM1 is a coupled earth system model to simulate climate processes and assessing environmental effects (Lee et al., 2020). CESM2 is model that allows for the investigation of multiple aspects of the Earth system, such as climatic variability, climate change, and the carbon cycle (Danabasoglu et al., 2020). The WACCM focuses on the study of atmospheric composition and its effects on climate and weather patterns. Lastly, the MIROC6 model, a part of the MIROC family of models, was used to examine various climate components and their interactions (Shiogama et al., 2019).

2.2 Method

2.2.1 Extreme Rainfall

Extreme rainfall was measured using climate indices established by the Expert Team on Climate Detection and Indices (ETTCDI). In this study, the R95p index was used, which calculated using Equations 1.

$$\mathrm{R95_p} = \sum_{w=1}^{w} \mathrm{RR_{wj}} \text{ where } \mathrm{RR_{wj}} > \mathrm{RR_{wn}}95 \qquad (1)$$

where w is the number of rainy days, $\mathrm{RR_{wj}}$ is the daily rainfall amount on the w-n day (with RR ≥ 1 mm) in a given period j, and $\mathrm{RR_{wn}}$ is the 95th percentile of rainfall on rainy days during the reference period.

2.2.2 ENSO and IOD Indices

ENSO were identified using the Ocean Niño Index (ONI), available at https://psl.noaa.gov/data/timeseries/monthly/ONI/. ONI reflects the SST anomaly in the Niño 3.4 region (5º N - 7º S dan 170º – 120º W), by subtracting the climatological monthly SST mean. The IOD was identified using Dipole Mode Index (DMI),

which can be accessed from https://psl.noaa.gov/gcos_wgsp/Timeseries/DMI/. DMI measures the difference in SST anomalies between the western (10º S - 0º N and 50º - 70º E) and southeastern (10º S – 0º N and 90º - 110º E) tropical Indian Ocean.

2.2.3 Model Evaluations

To determine which CMIP6 model best represents extreme rainfall to observational data, the models were evaluated using three statistical metrics: Pearson Correlation, Mean Error (ME), and Root Mean Squared Error (RMSE). Pearson Correlation measures how well the model predictions align with the observational data in a linear relationship. Mean Error (ME) identifies bias by calculating the average difference between the model predictions and the observations. RMSE checks how accurately the model captures the patterns and variability in the observed data. In addition, we used Rating Metric (RM) to rank the model. An RM value close to 1 indicates that the model performs well.

2.2.4 Relationship Between ENSO and IOD with Extreme Rainfall

In this study, linear regression was performed to analyze the spatial relationship of ENSO and IOD teleconnections with extreme rainfall during historical and future periods. Two scenarios of climate projections were used SSP2-4.5 and SSP5-8.5, the linear regression for the relationship is presented in Equation 2.

$$Y = A_1 + A_2X + \epsilon \quad (2)$$

where Y is the extreme rainfall variable (mm), A_1 is the constant, A_2 is the regression coefficient (mm/°C), X is the ENSO and IOD index (°C), and ϵ is the error term.

To analyze the independent influence of ENSO and IOD on extreme rainfall, partial regression was applied. This method removes the overlapping effects of one phenomenon on the other, allowing us to evaluate the impact of each event individually. For instance, the ENSO|IOD index represents the effect of ENSO after excluding the influence of IOD, while the IOD|ENSO index isolates the effect of IOD after accounting for ENSO (Kurniadi et al., 2021). This ensures that the analysis captures only the independent contribution of each event.

The study examined the teleconnection between extreme rainfall and both ENSO and IOD across all periods, quantifying changes in their relation over time. Changes in these relationships were then calculated by comparing future projections and historical data. To assess the significance of these changes, a student's t-test was performed at a 5% significance level.

3. RESULTS

3.1 Model Evaluation

In this model evaluation, five CMIP6 models were compared with observational data (GPM) to select the most accurate climate model for representing extreme rainfall (R95p). This evaluation is conducted for the SON season over the period from 2001 to 2014. The differences in average extreme rainfall during this period are presented in Figure 1.

There were differences in the average extreme rainfall between observational data (GPM) and CMIP6 models. It is evidence that the model tended to underestimate values compared to observational data, particularly in the regions of Sumatra, Kalimantan and Papua (Figure 1). This indicates that CMIP6 models are not yet fully capable of generating extreme rainfall as accurately as actual observations. Therefore, further evaluation of the models is necessary to identify the most accurate model for representing extreme rainfall

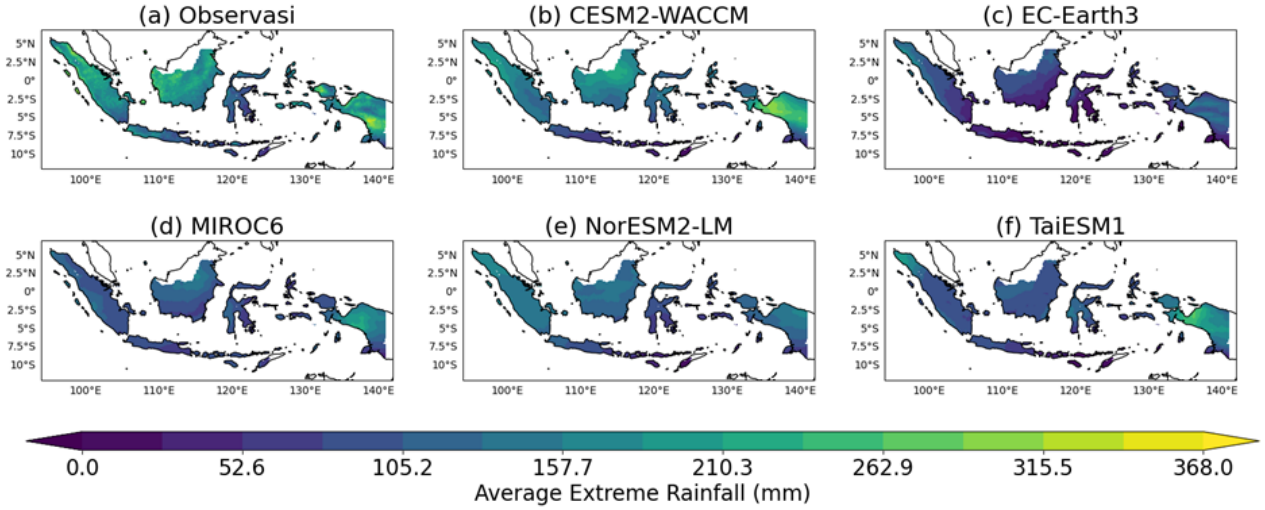

Figure 1. The average value of R95p using data from (a) GPM and (b-f) CMIP6 models during the period 2001-2014 for the September-October-November (SON) season.

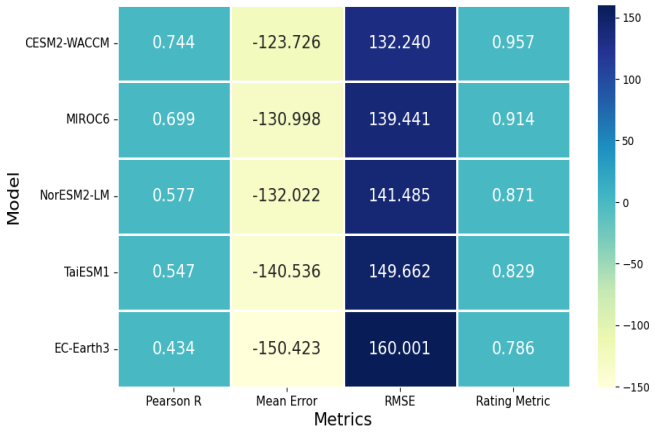

Figure 2. Evaluation of CMIP6 using the average R95p value with three parameters based on GPM data for the period 2001-2014 during the SON season.

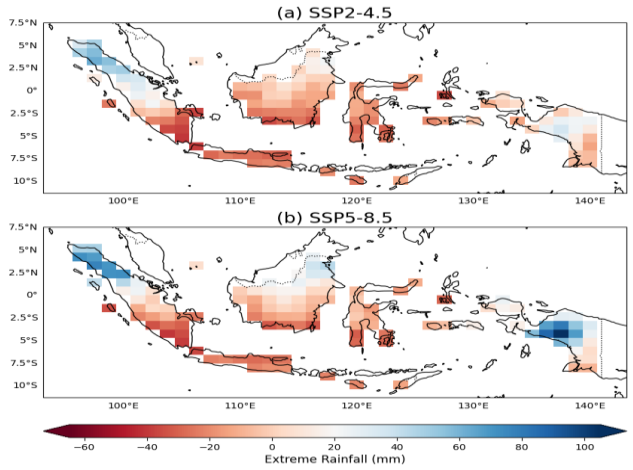

Figure 3. Changes in the average extreme rainfall (mm) in Indonesia during the SON season for the future period (2031-2090) based on the scenarios (a) SSP2-4.5 and (b) SSP5-8.5 relative to the reference period (1985-2014).

as observed in the data. The evaluation results showed that the CESM2-WACCM model is the best at representing extreme rainfall, with a Pearson Correlation value of 0.744, indicating a strong positive relationship between the model and observational data. The RMSE value of the model was 132.2, indicating a lower prediction error compared to other models, signifying that this model provides fairly accurate estimates for extreme rainfall. Despite the CESM2-WACCM model exhibiting the highest correlation compared to other models, we have not identified its application in Indonesia. The CMIP6 model, referenced by the IPCC and WMO, is the most prevalent, demonstrating the vulnerability of several cities in Southeast Asia to heightened precipitation and heat waves (Try and Qin, 2024).

3.2 Future Changes in Extreme Rainfall

Before analyzing the changes in the variability of extreme rainfall due to ENSO and IOD, it is necessary to examine the changes in extreme rainfall. The changes were calculated by subtracting the average extreme rainfall during the future period (2031-2090) from the historical period (1985-2014). Figure 3 shows the changes in average extreme rainfall during SON season, considering the SSP2-4.5 and SSP5-8.5 scenarios to compare with the reference period of the previous era. Based on Figure 3, changes in extreme rainfall in the future during SON season show variations either increase or decrease. Under the SSP2-4.5 scenario, projections indicated a reduction in increase up to 60 mm. Meanwhile, changes in extreme rainfall under the SSP5-8.5 scenario show a similar pattern to SSP2-4.5, but with northern Kalimantan and Papua experiencing increases of up to 90 mm. The changes are consistent with findings of Kurniadi et al., (2021), which reported an increased extreme rainfall in most the northern regions and a decreased in the southern part of Indonesia during SON. A further study on extreme precipitation projections in Indonesia indicates that Sumatra and Java will experience an increase in the length of the dry season by up to 40%, while extreme precipitation will occur in Kalimantan and mountainous areas in Papua, as predicted by the High-Resolution Model Inter-comparison Project (HigResMIP) model (Hariadi et al., 2024). However, our finding indicated differences from Kurniadi et al., (2024), which may be attributed to variations in data and the time periods used.

3.3 Future Changes in SST

In addition to examining changes in extreme rainfall in the future, it is also necessary to assess changes in SST (Sea Surface Temperature). The changes were calculated by subtracting the average SST of the future period (2031-2090) from the historical period (1985-2014). Based on Figure 4, there is a pattern of SST warming resembling El Niño in the Pacific Ocean. It is observed that SST increases are more significant in the central and eastern Pacific compared to the western Pacific. This finding is consistent with the research conducted by (Cai et al., 2015). The changes are expected to be more pronounced under the more extreme scenario (SSP5-8.5) compared to the SSP2-4.5 scenario. This larger warming could enhance the tendency for more frequent El Niño events, potentially impacting extreme weather patterns across various regions. The Indonesian Maritime Continent (IMC) is experiencing a warming trend in SST and ocean heat content that is significantly affecting marine eco-

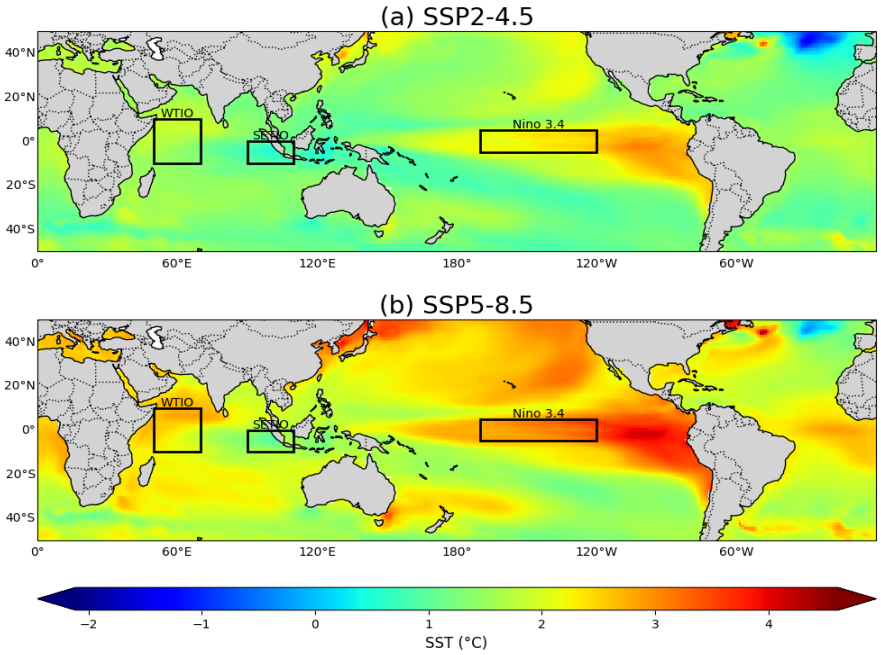

Figure 4. Changes in the average SST (°C) during the SON season between the future period (2031-2090) and the historical period (1985-2014) under the scenarios (a) SSP2-4.5 and (b) SSP5-8.5.

system. Warming at an average of 4.2^{x} 10^{8} Jm-1/decade over the past 30 years (Azis Ismail et al., 2023). In general, this study is consistent with previous research. In addition to the changes in SST in the Pacific Ocean, there are also changes in SST in the Indian Ocean. A warming pattern resembling a positive IOD is observed. This is consistent with the study by Cai et al. (2013), which shows greater warming in the western Indian Ocean compared to its surroundings. The changes are also anticipated to be more significant under the more extreme SSP5-8.5 scenario compared to the SSP2-4.5 scenario.

3.4 Changes in the Influence of ENSO on Extreme Rainfall

Generally, ENSO has more influence in the eastern region of Indonesia while IOD has more influence in the western region. This is because of the region's proximity to the Pacific and Indian oceans. Apart from that, there is a teleconnection between ENSO and IOD events and the areas they influence. The closer the source area of the increase or decrease in SST is to that area, the greater the impact of changes in SST. To assess the distribution of the influence of ENSO on extreme rainfall, a simple linear regression coefficient can be used. Additionally, the influence of ENSO-independent factors on extreme rainfall can be evaluated by removing the impact of IOD, which is calculated using partial regression. This analysis also considers regions showing significant influence, with hypothesis testing performed using the t-student test at a 5% significance level, marked by black dots on the map.

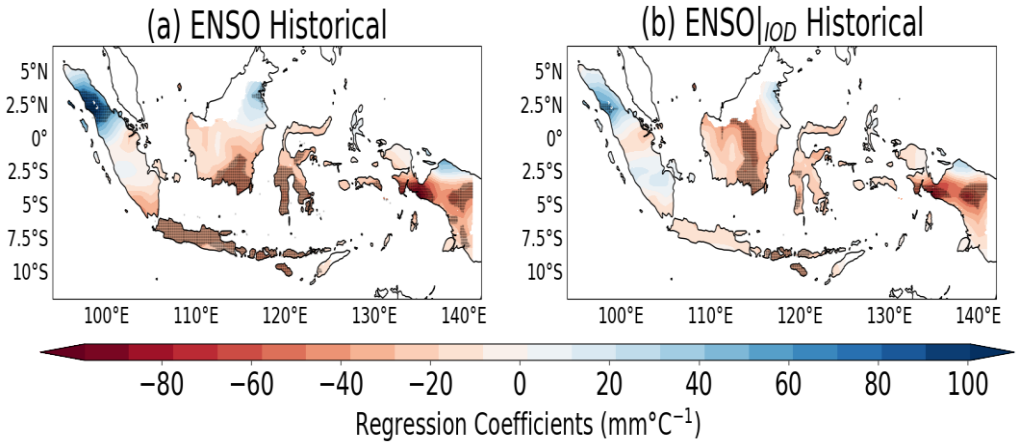

Figure 5. The influence of (a) ENSO and (b) ENSO-independent factors on IOD and extreme rainfall during the historical period (1985-2014) in the SON season.

Before examining the changes in the impact of ENSO on extreme rainfall in the future, it's crucial to review its influence during the historical period. Figure 5 illustrates the impact of ENSO and ENSO-independent factors on IOD regarding extreme rainfall during the period 1985-2014 for the SON season. It shows that extreme rainfall responses exhibit a negative relation-ship. This indicates that during the historical period, a one-degree increase in ONI corresponds to decrease in extreme rainfall in almost all regions of Indonesia. The increase in ONI values in the Pacific Ocean is related to increased evaporation and the formation of clouds over these waters, thereby affecting the Walker circulation. When El Nino occurs, rain clouds do not form in Java, South Kalimantan, South Sulawesi and parts of Papua, while North Sumatra and Aceh experience the opposite, namely increased cloud cover and extreme rainfall.

Before removing the IOD influence from ENSO, there is a significant relationship throughout Java with a regression coefficient of up to -40 mm/°C, meaning that in this region, a one-degree increase in ONI results in a decrease in extreme rainfall by up to 40 mm. Additionally, southern Kalimantan, southern Sulawesi and western Papua also show significant negative relationships. In contrast, northern Sumatra shows a significant positive relationship of up to 100 mm/°C, indicating that a one-degree increase in ONI leads to a 100 mm increase in extreme rainfall. After removing the IOD influence from ENSO, changes are observed. The previously significant relationships in Java and southern Sulawesi become non-significant. Conversely, significant negative relationships expand to central Kalimantan. Furthermore, the previously significant relationship in northern Sumatra becomes non-significant and reduces in magnitude. This suggests that IOD also plays a role in influencing extreme rainfall becomes smaller or even non-significant. After analyzing the impact of ENSO on extreme rainfall during the historical period, the next step is to analyze how these influences change in the future under the SSP2-4.5 and SSP5-8.5 scenarios. Changes are calculated by subtracting the regression coefficients of the future period from those of the historical period. These changes are also assessed for the impact of ENSO-independent factors on IOD, with a focus on regions showing significant relationship.

Based on Figure 6, there were changes in the influence of ENSO on extreme rainfall. In the near-future period, a negative change is observed across almost all regions of Indonesia except for Java. This negative change indicates that the future regression coefficients are lower compared to the historical period, suggesting that the negative relationship will strengthen in the future, while the positive relationship will weaken. The most significant change occurs in northern Kalimantan, reaching -80 mm/°C. This means that in northern Kalimantan in the future, there will be a decrease in extreme rainfall of 80 mm for every one-degree increase in ONI compared to the historical period.

Meanwhile, Java experiences a positive change of 20 mm/°C, meaning that in the future, the regression coefficient will be higher compared to the historical period, with each one-degree increase in ONI leading to a 20 mm increase in extreme rainfall. Compared to the far-future period, there are more positive changes such as those observed in Java, most of Kalimantan, and some other regions. According to the scenarios used, the changes were more significant under the SSP5-8.5 scenario compared to SSP2-4.5. After removing the IOD influence from ENSO, the changes exhibit a similar pattern to the changes in ENSO influence before the removal of IOD influence. In the far-future period under the SSP2-4.5 scenario, there are no significant, whereas under the SSP5-8.5 scenario, significant changes are

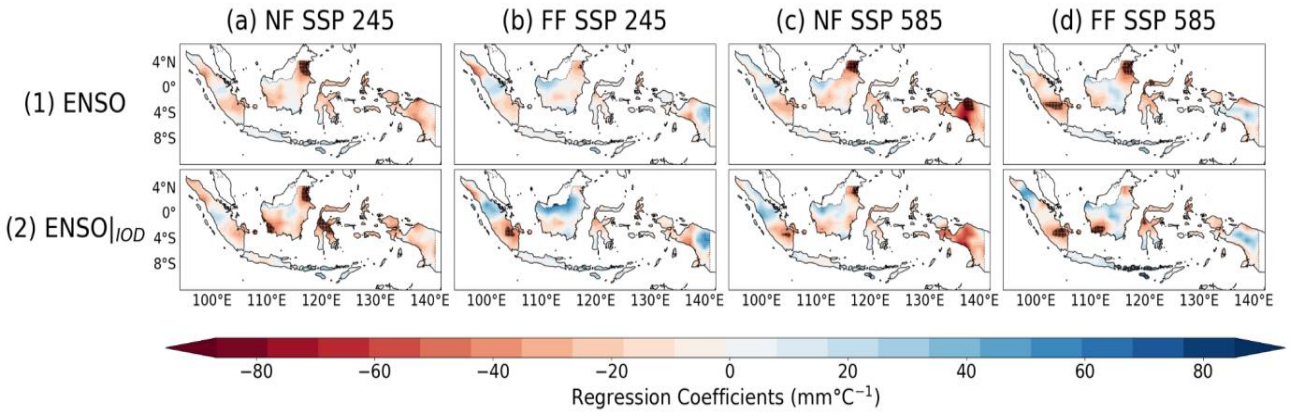

Figure 6. Changes in the influence of (1) ENSO and (2) ENSO-independent factors on IOD and extreme rainfall during the SON season for the periods (a and c) near-future (2031-2060) and (b and d) far-future (2061-2090) under the scenarios (a and b) SSP2-4.5 dan (c and d) SSP5-8.5.

observed in northern Kalimantan and southern Sumatra.

Negative changes indicating that the negative relationship between ENSO-independent factors and extreme rainfall will strengthen in the future. Significant changes are observed in northern Kalimantan and central Sulawesi, reaching -80 mm/°C. This means that in the near-future period, each one-degree increase in ONI will cause a decrease in extreme rainfall of 80 mm in these regions. Compared to the far-future period, there are more positive changes similar to the pattern seen in ENSO influence before removing the IOD effect.

3.5 Changes in the Influence of IOD on Extreme Rainfall

To assess the distribution of the influence of ENSO on extreme rainfall, simple linear regression coefficients can be used. Additionally, the influence of ENSO-independent factors on extreme rainfall can be assessed by removing the ENSO influence, calculated through partial regression. This analysis also considers regions exhibiting significant effects, with hypothesis testing performed using the t-student test at a 5% significance level, indicated by black dots on the map.

Figure 7 illustrates the influence of the IOD and IOD-independent factors on ENSO with respect to extreme rainfall during the historical period (1985-2014) for the SON season. The analysis reveals a negative relationship between extreme rainfall and the IOD in southern Indonesia, and a positive relationship in northern Indonesia. This indicates that historically, in southern Indonesia, each one-degree increase in the DMI index corresponds to a decrease in extreme rainfall, while in northern Indonesia, each one-degree increase in the DMI index corresponds to an increase in extreme rainfall. Before removing the influence of ENSO from the IOD for the SON season, significant relationships are observed on Java Island with a regression coefficient of up to -70 mm/°C. Additionally, southern Sumatra and southern Sulawesi also show significant relationships. Conversely, northern Indonesia exhibits significant positive relationships, particularly in northern Sumatra and northern Kalimantan, with coefficients up to 100 mm/°C.

After removing the influence of ENSO from the IOD, notable changes are observed. Southern Sulawesi, which previously showed a significant negative relationship, becomes non-significant. This indicates that ENSO also plays a role in influencing extreme rainfall in Indonesia. Subsequently, an analysis of the changes in the influence of IOD on extreme rainfall in the future under the SSP2-4.5 and SSP 5-8.5 scenarios is conducted, as shown in Figure 8. The changes are computed by subtracting the future period regression coefficients from the historical period coefficient. The analysis also considers the influence of IOD-independent factors on ENSO and identifies regions with significant effects.

Based on Figure 8, changes in the influence of the IOD on extreme rainfall are observed. During the near-future period, a negative shift is evident across most of Indonesia, except for Java Island under the SSP2-4.5 scenario. This negative change suggests that in the future, the negative regression coefficients will become stronger, while positive regression coefficients will weaken. The negative changes range from -90 to -90 mm/°C, with significant changes observed in northern Kalimantan. This indicates that in this region, there is a decrease of up to 90 mm in extreme rainfall for each one-degree increases in the DMI index. Conversely, the positive changes on Java Island range from 30 to 60 mm/°C, implying that in the near-future period, extreme rainfall on Java will increase by 30 to 60 mm for each one-degree increase in the DMI index.

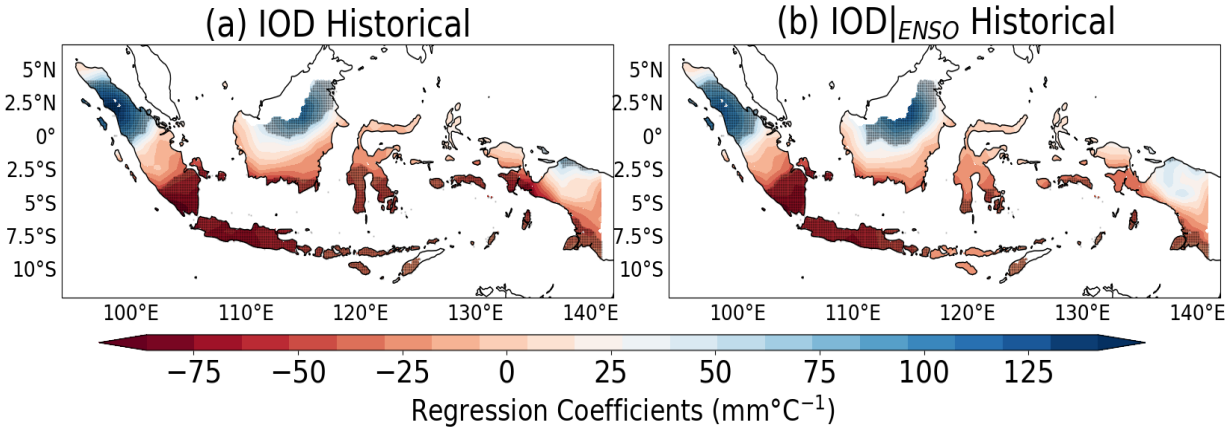

Figure 7. The influence of (a) IOD and (b) IOD-independent factors on ENSO and extreme rainfall during the historical period (1985-2014) in the SON season.

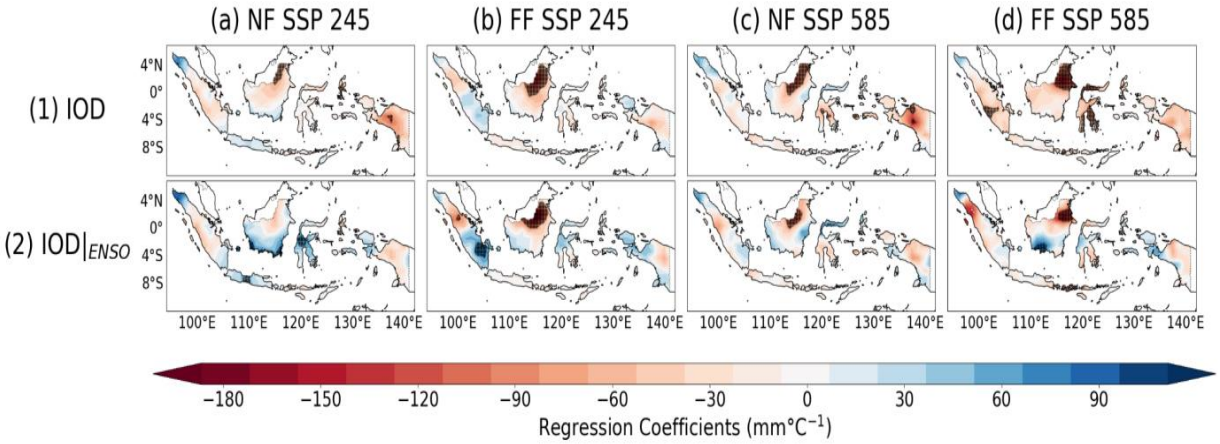

Figure 8. Changes in the influence of (1) IOD and (2) IOD-independent factors on ENSO and extreme rainfall during the SON season for the periods (a and c) near-future (2031-2060) and (b and d) far-future (2061-2090) under the scenarios (a and b) SSP2-4.5 dan (c and d) SSP5-8.5.

When comparing with the far-future period, distinct changes in pattern are noted. Southern Sumatra experienced a positive change of 20 to 60 mm/°C, indicating an increase in extreme rainfall by 20 to 60 mm for each one-degree increase in the DMI index in this region. Other regions exhibit patterns similar to those observed in the near-future period. The SSP5-8.5 scenario shows more significant changes compared to SSP2-4.5. For example, in the far-future period under SSP2-4.5, Sulawesi does not show significant changes, while under SSP5-8.5, significant changes are noted in both southern and northern Sulawesi.

After removing the influence of ENSO from the IOD, during the near-future period, southern Indonesia experiences positive changes, whereas northern Indonesia shows negative changes. This indicates that in the southern region, the future regression coefficients will increase, while in the northern region, the coefficient will decrease. Compared to the historical period, the negative influence in the southern region weakens in the future, while the positive influence in the northern region intensifies. This pattern is also observed in the far-future period, with more pronounced changes. Notably, after removing the ENSO influence, a shift from negative to positive values is observed in southern Kalimantan. The SSP5-8.5 scenario shows the most significant changes.

4. CONCLUSION

In this paper we showed future changes in extreme conditions in the IMC based on five climate models, namely CMIP6, TaiESM1, CESM2-WACCM, MIROC6, and NorESM2-LM. In general, our results are consistent with previous research. Most of IMC will get extreme dry spell and extreme rainfall only occur at Kalimantan and Papua. Furthermore, future climate changes will impact both extreme rainfall and Sea Surface Temperature (SST) and alter the influence of ENSO and IOD on extreme rainfall. During the near-future period, the teleconnections of ENSO and IOD with extreme rainfall show a negative shift across almost all regions, except for Java Island and northern Sumatra. This indicates that, in this period, negative relationships will become stronger while positive relationships will weaken, with the most significant changes occurring in northern Kalimantan, decrease of -80 mm/°C due to ENSO and -180 mm/°C due to IOD. In the far-future period, positive changes will become more widespread, especially in Kalimantan, suggesting that in this period, negative relationships will further weaken and positive relationships will strengthen.

The SSP5-8.5 scenario exhibits more significant changes compared to the SSP2-4.5 scenario. When evaluating the effects of ENSO and IOD independently, distinct patterns of change are observed. For ENSO viewed in isolation, the patterns are different yet similar to those observed before removing the IOD influence. Similarly, when examining IOD independently, significant changes are noted, such as a shift in the IOD in southern Kalimantan from negative to positive. This underscores the complexity of the interactions between ENSO and IOD in influencing extreme rainfall in Indonesia. So, these will be very important to weather and climate adaptations and development policies in Indonesia.

ACKNOWLEDGEMENT

The authors thank ITB for funding this research through the ITB 2024 program. We also extend our gratitude to Albert Sulaiman for his valuable discussions on extreme weather in the IMC and to M. Ridho Syahputra for his guidance in data processing.

REFERENCE

Amirudin, A.A., Salimun, E., Tangang, F., Juneng, L., Zuhairi, M., 2020. Differential Influences of Teleconnections from the Indian and Pacific Oceans on Rainfall Variability in Southeast Asia. Atmosphere 11. https://doi.org/10.3390/atmos11090886

Azis Ismail, F., Budiman, A., Yulihastin, E., Ratnawati, H., Surinati, D., Purwandana, A., Pranowo, W., Mujiasih, S., Hatmaja, R., Avianto, P., 2023. Warming of the Upper Ocean in the Indonesian Maritime Continent. pp. 489–496. https://doi.org/10.1007/978-981-19-9768-6_45

Cai, W., Santoso, A., Collins, M., Dewitte, B., Karamperidou, C., Kug, J.-S., Lengaigne, M., McPhaden, M.J., Stuecker, M.F., Taschetto, A.S., Timmermann, A., Wu, L., Yeh, S.-W., Wang, G., Ng, B., Jia, F., Yang, Y., Ying, J., Zheng, X.-T., Bayr, T., Brown, J.R., Capotondi, A., Cobb, K.M., Gan, B., Geng, T., Ham, Y.-G., Jin, F.-F., Jo, H.-S., Li, X., Lin, X., McGregor, S., Park, J.-H., Stein, K., Yang, K., Zhang, L., Zhong, W., 2021. Changing El Niño–Southern Oscillation in a warming climate. Nature Reviews Earth & Environment 2. https://doi.org/10.1038/s43017-021-00199-z

Cai, W., Santoso, A., Wang, G., Yeh, S.-W., An, S.-I., Cobb, K.M., Collins, M., Guilyardi, E., Jin, F.-F., Kug, J.-S., Lengaigne, M., McPhaden, M.J., Takahashi, K., Timmermann, A., Vecchi, G., Watanabe, M., Wu, L., 2015. ENSO and greenhouse warming. Nature Climate Change 5, 849–859. https://doi.org/10.1038/nclimate2743

Cai, W., Zheng, X.-T., Weller, E., Collins, M., Cowan, T., Lengaigne, M., Yu, W., Yamagata, T., 2013. Projected response of the Indian Ocean Dipole to greenhouse warming. Nature Geoscience 6, 999–1007. https://doi.org/10.1038/ngeo2009

Danabasoglu, G., Lamarque, J.-F., Bacmeister, J., Bailey, D.A., DuVivier, A.K., Edwards, J., Emmons, L.K., Fasullo, J., Garcia, R., Gettelman, A., Hannay, C., Holland, M.M., Large, W.G., Lauritzen, P.H., Lawrence, D.M., Lenaerts, J.T.M., Lindsay, K., Lipscomb, W.H., Mills, M.J., Neale, R., Oleson, K.W., Otto-Bliesner, B., Phillips, A.S., Sacks, W., Tilmes, S., van Kampenhout, L., Vertenstein, M., Bertini, A., Dennis, J., Deser, C., Fischer, C., Fox-Kemper, B., Kay, J.E., Kinnison, D., Kushner, P.J., Larson, V.E., Long, M.C., Mickelson, S., Moore, J.K., Nienhouse, E., Polvani, L., Rasch, P.J., Strand, W.G., 2020. The Community Earth System Model Version 2 (CESM2). Journal of Advances in Modeling Earth Systems 12, e2019MS001916. https://doi.org/10.1029/2019MS001916

Deshmukh, C.S., Julius, D., Desai, A.R., Asyhari, A., Page, S.E., Nardi, N., Susanto, A.P., Nurholis, N., Hendrizal, M., Kurnianto, S., Suardiwerianto, Y., Salam, Y.W., Agus, F., Astiani, D., Sabiham, S., Gauci, V., Evans, C.D., 2021. Conservation slows down emission increase from a tropical peatland in Indonesia. Nature Geoscience 14, 484–490. https://doi.org/10.1038/s41561-021-00785-2

Hamdi, S., Rizal, S., Shibata, T., Darmawan, A., Irfan, M., Sulaiman, A., 2024. The dispersion of smoke haze from peatland fires over South Sumatra during the moderate El Niño of 2023. Natural Hazards. https://doi.org/10.1007/s11069-024-06857-x

Hariadi, M.H., van der Schrier, G., Steeneveld, G.-J., Sutanto, S.J., Sutanudjaja, E., Ratri, D.N., Sopaheluwakan, A., Klein Tank, A., 2024. A high-resolution perspective of extreme rainfall and river flow under extreme climate change in Southeast Asia. Hydrology and Earth System Sciences 28, 1935–1956. https://doi.org/10.5194/hess-28-1935-2024

Hermawan, E., Lubis, S.W., Harjana, T., Purwaningsih, A., Risyanto, Ridho, A., Andarini, D.F., Ratri, D.N., Widyaningsih, R., 2022. Large-Scale Meteorological Drivers of the Extreme Precipitation Event and Devastating Floods of Early-February 2021 in Semarang, Central Java, Indonesia. Atmosphere 13. https://doi.org/10.3390/atmos13071092

Hidayat, R., Ando, K., 2014. RAINFALL VARIABILITY OVER INDONESIA AND ITS RELATION TO ENSO/IOD: ESTIMATED USING JRA-25/JCDAS. Agromet 28, 1–8. https://doi.org/10.29244/j.agromet.28.1.1-8

Kurniadi, A., Weller, E., Min, S.-K., Seong, M.-G., 2021. Independent ENSO and IOD impacts on rainfall extremes over Indonesia. International Journal of Climatology 41, 3640–3656. https://doi.org/10.1002/joc.7040

Kurniadi, A., Weller, E., Salmond, J., Aldrian, E., 2024. Future projections of extreme rainfall events in Indonesia. International Journal of Climatology 44, 160–182. https://doi.org/10.1002/joc.8321

Lee, W.-L., Wang, Y.-C., Shiu, C.-J., Tsai, I., Tu, C.-Y., Lan, Y.-Y., Chen, J.-P., Pan, H.-L., Hsu, H.-H., 2020. Taiwan Earth System Model Version 1:

description and evaluation of mean state. Geoscientific Model Development 13, 3887–3904. https://doi.org/10.5194/gmd-13-3887-2020

Lestari, S., King, A., Vincent, C., Karoly, D., Protat, A., 2019. Seasonal dependence of rainfall extremes in and around Jakarta, Indonesia. Weather and Climate Extremes 24, 100202. https://doi.org/10.1016/j.wace.2019.100202

Liang, J., Catto, J.L., Hawcroft, M.K., Tan, M.L., Hodges, K.I., Haywood, J.M., 2023. Borneo Vortices in a warmer climate. npj Climate and Atmospheric Science 6, 2. https://doi.org/10.1038/s41612-023-00326-1

Lisnawati, Taufik, M., Dasanto, B.D., Sopaheluwakan, A., 2022. Fire Danger on Jambi Peatland Indonesia based on Weather Research and Forecasting Model. Agromet 36, 1–10. https://doi.org/10.29244/j.agromet.36.1.1-10

Lubis, S.W., Hagos, S., Hermawan, E., Respati, M.R., Ridho, A., Risyanto, Paski, J.A.I., Muhammad, F.R., Siswanto, Ratri, D.N., Setiawan, S., Permana, D.S., 2022. Record-Breaking Precipitation in Indonesia's Capital of Jakarta in Early January 2020 Linked to the Northerly Surge, Equatorial Waves, and MJO. Geophysical Research Letters 49,e2022GL101513. https://doi.org/10.1029/2022GL101513

Saidah, H., Sulistiyono, H., Negara, I.D.G.J., 2023. Comparison of Suitable Drought Indices for Over West Nusa Tenggara, in: Kristiawan, S.A., Gan, B.S., Shahin, M., Sharma, A. (Eds.), Proceedings of the 5th International Conference on Rehabilitation and Maintenance in Civil Engineering. Springer Nature Singapore, Singapore, pp. 587–600.

Setiawan, R.Y., Susanto, R.D., Horii, T., Alifdini, I., Siswanto, E., Sari, Q.W., Wirasatriya, A., Aryudiawan, C., 2024. The Fujiwhara effect on ocean biophysical variables in the southeastern tropical Indian Ocean region. Journal of Marine Systems 245, 103990. https://doi.org/10.1016/j.jmarsys.2024.103990

Shiogama, H., Abe, M., Tatebe, H., 2019. MIROC MIROC6 model output prepared for CMIP6 ScenarioMIP. https://doi.org/10.22033/ESGF/CMIP6.898

Sulaiman, A., Osaki, M., Takahashi, H., Yamanaka, M.D., Susanto, R.D., Shimada, S., Kimura, K., Hirano, T., Wetadewi, R.I., Sisva, S., Kato, T., Kozan, O., Kubo, H., Awaluddin, A., Tsuji, N., 2023. Peatland groundwater level in the Indonesian maritime continent as an alert for El Niño and moderate positive Indian Ocean dipole events. Scientific Reports 13, 939. https://doi.org/10.1038/s41598-023-27393-x

Susanto, R.D., Aldrian, E., 2003. Identification of Three Dominant Rainfall Regions Within Indonesia and Their Relationship to Sea Surface Temperature. International Journal of Climatology, pp. 1435–1452. https://doi.org/10.1002/joc.950

Sutardi, Apriyana, Y., Rejekiningrum, P., Alifia, A.D., Ramadhani, F., Darwis, V., Setyowati, N., Setyono, D.E., Gunawan, Malik, A., Abdullah, S., Muslimin, Wibawa, W., Triastono, J., Yusuf, Arianti, F.D., Fadwiwati, A.Y., 2023. The Transformation of Rice Crop Technology in Indonesia: Innovation and Sustainable Food Security. Agronomy 13. https://doi.org/10.3390/agronomy13010001

Trismidianto, Andarini, D.F., Muharsyah, R., Purwaningsih, A., Risyanto, Nauval, F., Fathrio, I., Harjupa, W., Nuryanto, D.E., Harjana, T., Satiadi, D., Saufina, E., Praja, A.S., 2023. Interactions among Cold Surge, Cross-Equatorial Northerly Surge, and Borneo Vortex in influencing extreme rainfall during Madden–Julian oscillation over the Indonesia Maritime Continent. Meteorology and Atmospheric Physics 135.

Try, S., Qin, X., 2024. Evaluation of Future Changes in Climate Extremes over Southeast Asia Using Downscaled CMIP6 GCM Projections. Water 16. https://doi.org/10.3390/w16152207

Yulianto, F., Khomarudin, R., Hermawan, E., Budhiman, S., Sofan, P., Chulafak, G., Nugroho, N., Prima, R., Nugroho, G., Suwarsono, S., Priyanto, E., Listi, H., Setiyoko, A., Sakti, A., 2023. The development of the Raster-based Probability Flood Inundation Model (RProFIM) approach for flood modelling in the upstream Citarum Watershed, West Java, Indonesia. Natural Hazards 117. https://doi.org/10.1007/s11069-023-05933-y

Yulihastin, E., Fathrio, I., Sulaiman, A., Hatmaja, R.B., Suaydhi, Satyawardhana, H., Nauval, F., Nugroho, D., Djamaluddin, T., Pranowo, W.S., Bramawanto, R., Basit, A., Mujiasih, S., Ismail, M.F.A., Lestari, S., Ratnawati, H.I., Nugroho, J.T., Nuryanto, D.E., 2023. Propagation of tropical squall line-induced storm coastal inundation episodes in Java-Bali, Indonesia. Heliyon 9, e19804. https://doi.org/10.1016/j.heliyon.2023.e19804